WOOD RESEARCH doi.org/10.37763/wr.1336-4561/68.3.488501
ISSN 1336-4561 e-ISSN 2729-8906
68(3): 2023 488-501 pp.

DETERMINATION OF UREA-FORMALDEHYDE RESIN CONTENT IN POPLAR FIBER BASED ON HYPERSPECTRAL TECHNIQUES

CHUNMEI YANG[1], ZANBIN ZHU[1,2], TONGBIN LIU[1], BO XUE[1],
WEN QU[1], TINGTING WANG[1]

[1]NORTHEAST FORESTRY UNIVERSITY, CHINA
[2]XINYANG AGRICULTURE AND FORESTRY UNIVERSITY, CHINA

(RECEIVED APRIL 2023)

ABSTRACT

In this experiment, poplar fibers containing 0%, 2%, 4%, 6%, 8%, 10%, 12%, 14%, 16%, 18%, 20%, 25% and 30% of urea-formaldehyde resin were prepared. A model for the detection of urea-formaldehyde resin content in poplar fibers was established by the hyperspectral near-infrared imaging system combined with relevant algorithms. The spectral images of poplar fibers containing different contents of urea-formaldehyde (UF) resin were measured separately using hyperspectral imager. The results of four preprocessing methods, namely mean centering (MC), multiple scattering correction (MSC), standard normal variables (SNV) and first-order derivative (1-Der) were analyzed, and the optimal preprocessing method was selected as SNV. The band combinations with the highest correlation with the urea-formaldehyde resin content were compared and analyzed with the full-band model to establish the partial least squares regression (PLSR) model. The experimental results show that the hyperspectral imaging system combined with the corresponding algorithm can achieve rapid detection of UF resin content in poplar fibers, and the results of this study provide technical support and theoretical reference for determination of resin content in ultra-thin fiberboard production. The method is an innovative model for the determination of UF resin in wood fibers.

KEYWORDS: Fiberboard, urea-formaldehyde resin, hyperspectral, characteristic wavelength.

INTRODUCTION

During the production of fiberboard, the content of urea-formaldehyde (UF) resin in poplar fibers is a key factor in the mechanical properties as well as the environmental performance of fiberboard (Zhang et al. 2023, Zou et al. 2020). During the hot pressing process,

the wood fibers with the addition of UF resin are closely bonded to the UF resin under high temperature and pressure, thus forming a board with certain mechanical strength (Thoemen et al. 2003, 2006, Garcia et al. 2005). Therefore, the content of the UF resin in the wood fibers must be precisely controlled and distributed as evenly as possible. Tang et al. (2022) investigated the effect of resin content on the properties of high density fiberboard (HDF) using poplar fiber and isocyanate gum as raw materials. The results show that with the resin content increasing from 3% to 10%, the water resistance and mechanical properties of HDF are gradually enhanced. When the resin content is 10%, the board has the highest binding strength and the best performance. With the further increase of resin content, it is easy to cause bulges in the process of hot pressing. so that its mechanical properties decline.

The ultra-thin fiberboard of 0.8 mm thickness in this study, due to its thinner thickness, the influence of the UF resin content on its performance is more critical. The ultra-thin fiberboard with uniform content of UF resin has a flat and smooth surface with more uniform color (Fig. 1a). If too much UF resin accumulates in the fiber, the moisture in the UF resin will increase the moisture content of the raw material, and when it enters the hot pressing process, it will produce bulging defects, spots, and the release of formaldehyde after the UF resin is heated will also increase (Fig. 1b); If too little UF resin accumulates in poplar wood fibers, the raw material will not be easily compacted, and the man-made board will easily produce defects such as delamination, uneven slab molding, and poor mechanical properties (Fig. 1c).

(a) (b) (c)

Fig. 1: a) qualified fiberboard, b) glue spot, c) poor bonding.

Continuous hot presses are currently used for the production of fiberboard to achieve continuous and uninterrupted production. The content of UF resin in poplar fibers is extremely important for the adjustment of the process parameters of the press, and it is crucial to quickly detect defects in gluing technology and adjust the process in time (Ncube 2012, Rofii et al. 2014). Therefore, it is of great practical value to quickly and accurately determine the content of UF resin in wood fibers before the hot pressing of fibers, so that the parameters of the gluing system can be adjusted in time. Research has also been conducted on the gluing system of fiberboard and the composition of the adhesive (Hata et al. 1989, Carvalho et al. 1998). Meng (2011) studied the complexity, nonlinearity, hysteresis and dynamics of fiberboard gluing systems. Jakes et al. (2019) probed adhesive penetration including the inflow of adhesive into the micron-sized voids of wood and penetration into the polymer composition of the wood cell wall layer using X-ray computed tomography (XCT) and X-ray fluorescence microscopy (XFM).

In summary, most of the related researchers focus on the effect of adhesive content on the performance of fiberboard and the bonding mechanism to improve its mechanical properties. This study combines hyperspectral technology to perform rapid detection of UF resin content in wood fibers by using the characteristics of inconsistent chemical composition of UF resin and poplar fibers. In recent years, spectroscopic detection has been applied in the field of agricultural and forestry engineering (Lorente et al. 2013, Magwaza et al. 2012, Zhu et al. 2013, Cleve et al. 2000). Hyperspectral studies have been used for wood species identification and detection, and more scholars have used hyperspectral detection to determine various indicators such as tree species, density, and moisture content (Liu et al. 2014, Tsuchikawa et al. 2015). Fujimoto et al. (2012) collected NIR spectra of larch at different moisture contents and analyzed wood density using PLS, and the results showed that wood density prediction using NIR spectroscopy was not affected by moisture conditions. Fernandes et al. (2013) used hyperspectral imaging to measure density profiles at the growth year scale of trees. The relationship between spectral reflectance and its density value was modeled by partial least squares regression analysis using hyperspectral imaging to measure the reflectance of wood samples. Ma et al. (2018) used NIR hyperspectral imaging combined with partial least squares regression analysis to assess the hardness (modulus of elasticity) and fiber thickness of wood. Reis et al. (2019) used multivariate statistical analysis to develop a NIR spectral model to successfully distinguish between natural and planted wood. Stefansson et al. (2021) combined the spectral data with a partial least squares regression method to map the absorbance data of each sample to the moisture content distribution of the samples at different time steps during the drying process. Jiang et al. (2007) used NIR spectroscopy analyzed the resin content, the calibration model of resin content was established by partial least squares (PLS) regression. Özparpucu et al. (2022) Combined FTIR spectroscopy and rheology measurements of the curing of melamine formaldehyde (MUF) adhesives as influenced by different wood extracts.

Poplar fibers are composed of cellulose, hemicellulose, and lignin, which are mainly composed of C, H, and O. The N content is extremely low, about 0.1-1%. UF resin is a thermosetting resin formed by the condensation of urea $CH_4\ N_2\ O$ and formaldehyde $CH_2\ O$ under the action of a catalyst (alkaline or acidic catalyst) to form an initial resin, followed by the action of a curing agent or additives. There is a big difference in the chemical composition of poplar fiber and the content of hydrogen-containing groups (O-H, N-H, C-H) of organic molecules in UF resins. Therefore identification can be based on NIR spectral features.

There are few quantitative tests for UF resin in poplar fibers after gluing. This study combines the characteristics of hyperspectral for rapid quantitative detection of UF resin content in wood fibers, which provides a reference value for timely adjustment of gluing process of industrial high-density fiberboard.

MATERIAL AND METHODS

Materials

The poplar fiber and UF glue used in this experiment were obtained from the test production line of ultra-thin boards in Jining, Shandong, China. In this test, pure poplar fiber was mixed with UF resin in proportion to its weight by weighing on a balance, the UF resin

after mixing was 0% (pure poplar fiber), 2%, 4%, 6%, 8%, 10%, 12%, 14%, 16%, 18%, 20%, 25%, 30% and 100% (UF), for a total of 14 samples with different resin contents to be tested.

In order to obtain relatively uniform poplar fiber with different content of UF, the method of glue spraying was used. The fiber glue machine structure is shown in Fig. 2. The unglued poplar fibers are placed in the mixing drum of the apparatus and the UF is mixed with high pressure air in the duct. The UF is atomised by the atomiser and the poplar fibers are rotated by the plough mixer. Poplar fibers with different UF contents are configured by matching different weights of fibers and UF.

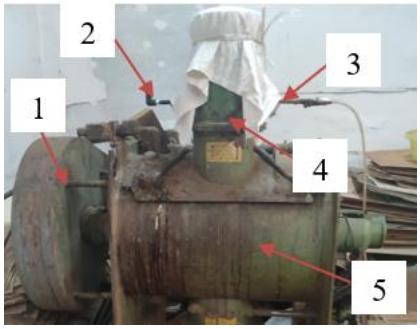

Fig. 2: Fiber glue machine: (1) electromotor, (2)UF pipeline , (3) high pressure airline , (4) atomizer, (5) plough mixer.

The lens used in this experiment was FX17 (Specim FX17, Finland), as shown in Fig. 3, with a wavelength range of 900-1700 nm. Since hyperspectroscopy utilizes the principle of diffuse reflection, the samples were spread evenly on black hard paper in order to reduce errors. The parameters of the hyperspectral camera used for the experiments are shown in Tab. 1.

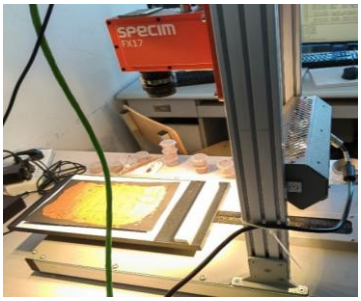

Fig. 3: Detection platform of hyperspectral camera.

Tab. 1: Related parameters of hyperspectral measurement system.

Instrument manufacturers	Camera model	Spectral range	Spectral resolution (FWHM)	Spectral sampling/pixel	Spectral bands
Specim	FX17	900 nm -1700 nm	8 nm	3.5 nm	224

Methods

The parameters of the system were set as 2 mm/s for the electronically controlled stage movement, 15 ms for the camera exposure time, and 20 cm for the object distance, followed by black and white plate image acquisition, and then hyperspectral image information was acquired for the samples. Due to the presence of dark currents and uneven distribution of light sources, the acquired hyperspectral images contain a large amount of noise. In order to

eliminate the effects of uneven illumination and external environmental factors, the hyperspectral image data need to be corrected in black and white before data processing. The black-and-white correction was then performed on the original image according to Eq. 1:

$$R\% = (R_0 - R_B) / (R_W - R_B) \times 100\% \quad (1)$$

where: R_0 is the reflectance spectral image; R_B is the image of the blackboard with the lens cap on, R_W is the image of the white board with the teflon white board on, and R is the corrected diffuse reflectance spectral image (Shao et al 2019).

The raw spectral information was collected using ENVI (Classic 5.3 + IDL 8.5) software and the spectra for a given content were converted to ASCII information by ENVI software and corrected for black and white. The raw spectral sample curves for UF are shown in Fig. 4a, while the pure poplar fiber spectral sample curves are shown in Fig. 4b.

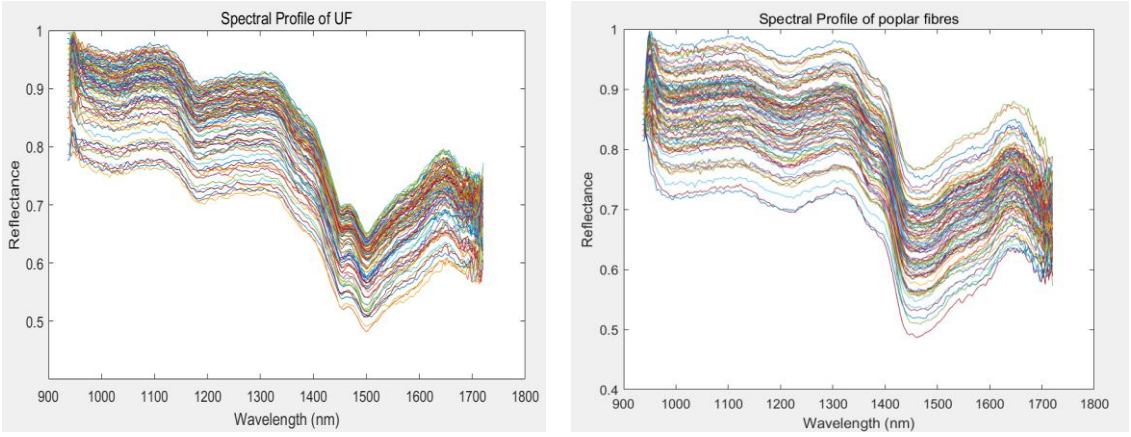

(a) (b)

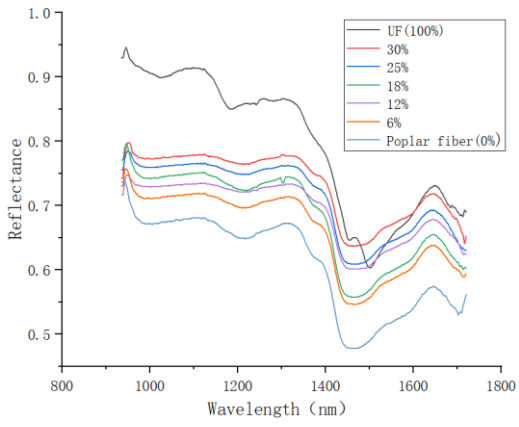

(c)

Fig. 4: a) Spectral profile of UF, b) spectral profile of poplar fiber, c) average spectra of poplar fiber with different UF resin contents.

The average spectra for different UF resin contents were obtained using Origin 2021 and are shown in Fig. 4c. The average spectral curves for UF resin contents have the same curve

trend. The spectral curves of UF resin are different from those of pure poplar fiber, and their spectral reflectance has different characteristics in the wavelength range of 1350-1550 nm, and their spectral absorption values have different reflectance. The spectral data were pre-processed, screened for characteristic wavelengths and modelled using MATLAB 2020a, Origin 2021 and Python3.7 software. So that the content of UF resin in poplar fiber can be quantitatively and quickly detected based on the spectral data.

Sample division and pre-processing of spectral information

The sample was divided equally into 9 different areas on black hard paper, and the average spectra of about 100 pixel points in each area were randomly selected as the spectral information of that area, 10 times, i.e. 90 spectra for each content were selected. A total of 1260 spectral samples were taken for the overall test article. The Kennard-Stone (K-S) method was used to divide all the spectral samples, and a ratio of 2:1 between the calibration set spectral data and the prediction set spectral data was used to obtain a calibration set of 840 items and a prediction set of 420 items. In combination with the requirements of spectral detection, the spectral information needs to be pre-processed so as to reduce the errors in the model data. In conjunction with the spectral analysis associated with wood type detection this experiment utilises mean-centred (MC), multiple scattering correction (MSC), standard normal variance transformation (SNV) and first order derivative (1-Der) to pre-process the spectral data for this experiment.

RESULTS AND DISCUSSION

The PLSR method was used to establish the relationship between UF resin content and NIR spectra. The final PLSR model performance was evaluated for R^2c, RMSEC, R^2p and RMSEP to assess the accuracy of the model.

$$R^2C = \frac{\sum_{i=1}^{n}(Y_i - \bar{y})^2}{\sum_{i=1}^{n}(y_i - \bar{y})^2} \quad (2) \qquad R^2P = \frac{\sum_{i=1}^{m}(Y_i - \bar{y})^2}{\sum_{i=1}^{m}(y_i - \bar{y})^2} \quad (3)$$

$$RMSEC = \sqrt{\frac{\sum_{i=1}^{n}(Y_i - y_i)^2}{n-1}} \quad (4) \qquad RMSEP = \sqrt{\frac{\sum_{i=1}^{m}(Y_i - y_i)^2}{m-1}} \quad (5)$$

where: y_i is the measured value of the reference method; Y_i is the predicted value of NIR model; $\bar{y}$ is the average value of y_i in the calibration set; n is the number of calibration set samples; m is the number of samples in the prediction set.

The larger the R^2 is, the better the model fitting effect. RMSEC (Root mean square error of calibration) is the deviation between the true and predicted values in the calibration model, and RMSEP (Root mean square error of prediction) is the deviation between the true and predicted values in the prediction model (Liu et al. 2016). The results of the PLSR (partial least squares regression) model evaluation of the UF content after the four pre-processed spectral data are

shown in Tab. 2.

Tab. 2: Evaluation results of UF content by PLSR regression model under different pretreatment methods.

Pretreatment methods	Number of principal factors	Calibration set		Prediction set	
		R^2c	RMSEC	R^2p	RMSEP
None pre-processing	8	0.916	1.226	0.894	1.870
Mean centering (MC)	8	0.929	1.153	0.903	1.678
Multiplicative scatter correction (MSC)	7	0.934	0.891	0.912	1.336
Standard normal variate (SNV)	7	0.959	0.805	0.937	1.275
1st derivative (1-Der)	2	0.864	1.465	0.831	2.134

As can be seen from Tab. 2, the PLSR model for the UF resin content was established after different pre-processing of the spectral data, where the R^2c and R^2P values increased from 0.916 and 0.894 to 0.959 and 0.937, respectively, compared to the data without pre-processing. The results indicate that pre-processing with SNV eliminated the effects of fiber solid particle size, surface scattering and light range variations on the diffuse reflectance spectrum. Therefore, SNV was chosen as the spectral pre-processing algorithm for this study.

The results of this experiment to screen the characteristic wavelengths associated with the indicators of UF resin content in poplar fiber using the SPA and CARS algorithms, which reflect sensitivity to UF resin content using the SPA method, are shown in Fig. 5. From Fig. 5a it can be seen that the RMSE value reaches a minimum when the number of variables is 29, after which it tends to level off overall. Fig. 5b shows the specific distribution of these 29 wavelengths. Details of the characteristic bands screened using the SPA method are shown in Tab. 3.

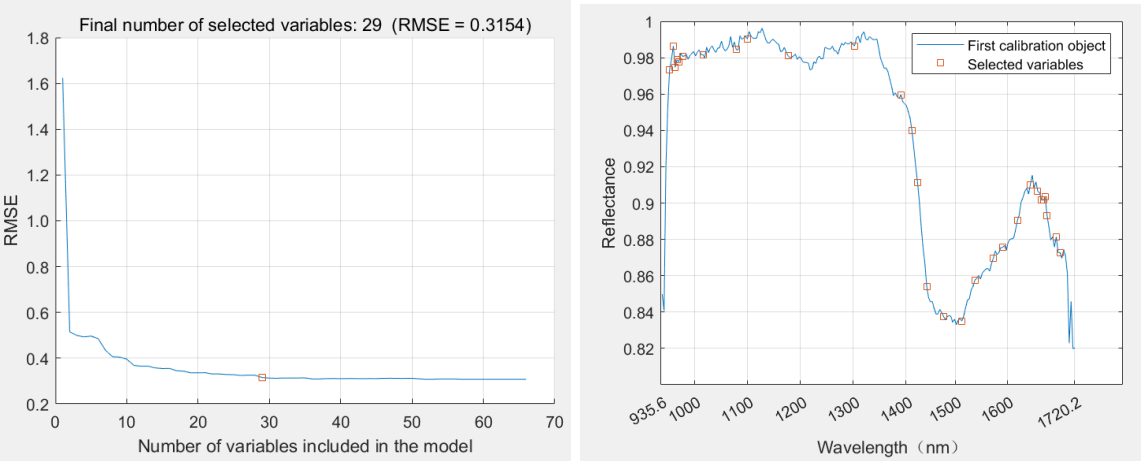

(a) (b)

Fig. 5: a) Number of characteristic wavelengths selected by SPA algorithm; b) detailed position of characteristic wavelengths.

Competitive Adaptive Re-weighted Sampling (CARS) is a method that combines Monte Carlo and PLS model regression coefficients to filter the characteristic wavelengths. The distribution of the 55 characteristic wavelengths obtained after pre-processing the data by

SNV using the CARS algorithm is shown in Tab. 3. From Fig. 6a it can be seen that the number of preferred variables all decrease exponentially with the number of Monte Carlo iterations under the exponential decay function, and from Fig. 6b it can be seen that the RMSECV value decreases and then increases and has the smallest value at the number of runs of 17. Fig. 6c shows that, overall, the RMSECV values for the first 20 samples are relatively low, increasing with the number of samples, indicating that information or noise not related to the fiber UF resin content is being added to the reflectance spectrum, resulting in increased values.

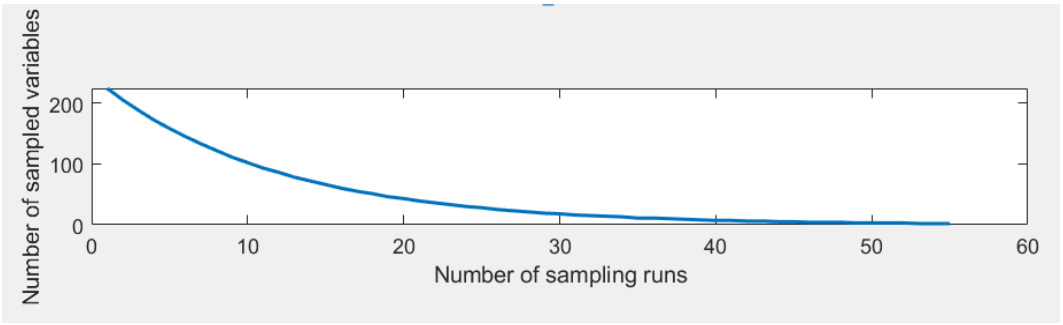

(a)

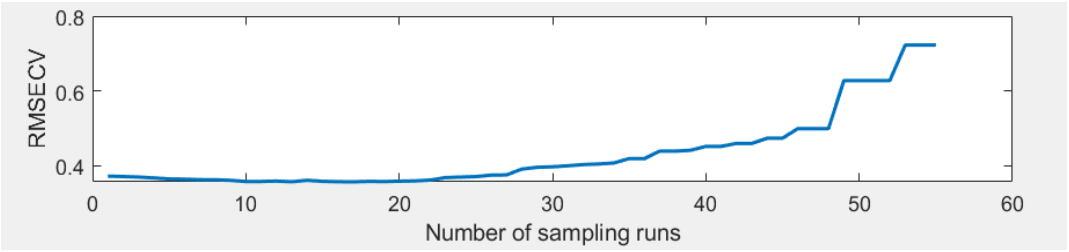

(b)

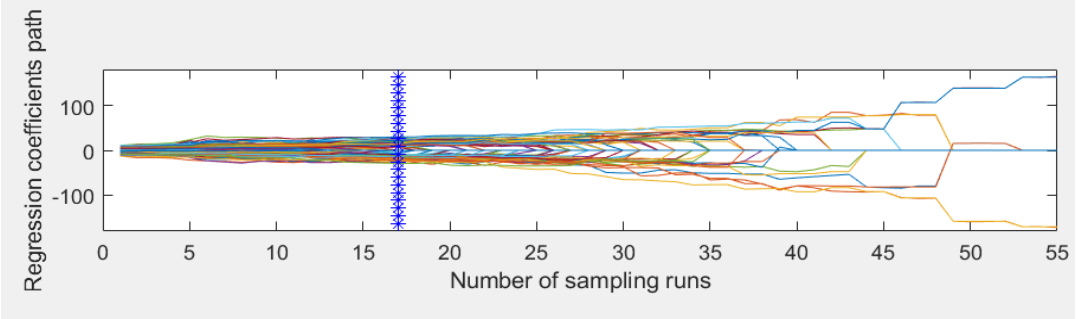

(c)

Fig. 6: a) Variation diagram of number of wavebands variables, b) variation diagram of RMSECV, c) path diagram of regression coefficients of variables.

Tab. 3: Characteristic wavelengths selected by SPA and CARS.

Method	Number of wavelengths	Characteristics wavelengths
Successive projections algorithm （SPA）	29	949.4、956.3、959.8、963.3、966.7、973.7、1011.8、1074.3、1095.2、1171.9、1298.1、1386.1、1407.3、1417.9、1435.5、1467.4、1502.8、1527.7、1563.2、1581.0、1609.5、1634.4、1648.7、1655.9、1659.4、1663.0、1666.6、1684.4、1691.6、

Competitive adaptive reweighed sampling (CARS)	55	991.0、1004.8、1011.8、1015.2、1022.2、1091.7、1109.1、1126.5、1140.5、1150.9、1154.4、1168.4、1178.9、1182.4、1189.4、1217.4、1220.9、1227.9、1259.4、1298.1、1361.4、1389.6、1396.7、1417.9、1432.0、1435.5、1439.1、1442.6、1449.7、1453.2、1470.9、1474.5、1478.0、1481.6、1499.3、1502.8、1506.4、1517.0、1524.1、1534.8、1538.3、1541.9、1549.0、1563.2、1566.8、1573.9、1581.0、1584.6、1588.1、1595.2、1598.8、1602.3、1666.6、1680.9、1684.4、

In this experiment, a PLSR model was developed to predict the content of UF resin in fibers based on 224 wavelengths in all bands pre-treated by SNV and 29 characteristic wavelengths screened by SPA and 55 characteristic wavelengths screened by CARS. The model performance was evaluated in terms of four indicators, R^2c, RMSEC, R^2p and RMSEP. As can be seen from Tab. 3, the vast majority of the wavelengths screened by the SPA were in the 950 nm to 1000 nm and 1300 nm to 1700 nm regions, while the CARS algorithm identified a relatively large number of characteristic wavelengths, mostly concentrated in the 1300 nm to 1700 nm and a small number in the 1100-1200 nm region. As can be seen from Tab. 4, the CARS algorithm selected 24.55% of the 224 feature bands, which shortens the computation time and the number of variables, while the prediction performance is still excellent.

Tab. 4: The results with PLSR model based on different variable selection methods.

Method	Number of wavelengths	Number of principal factors	Calibration set		Prediction set	
			R^2c	RMSEC	R^2p	RMSEP
SNV-Full	224	7	0.959	0.805	0.937	1.275
SNV-SPA	29	3	0.931	1.131	0.906	1.436
SNV-CARS	55	7	0.941	0.865	0.921	1.305

In summary, hyperspectroscopy combined with correlation algorithms is a good way to achieve rapid detection of UF resin content in poplar fibers, which, in combination with previous studies, is mostly determined using fluorescent labelling combined with electron microscopy and other methods (Xing et al. 2005, Javed et al. 2015, Kekkonen et al. 2014). Xing et al. (2004) measured the content of UF resin in wood fibers in MDF using confocal laser scanning microscopy and image analysis techniques. Thus, the extent of distribution of the binder on the fiber surface and the degree of distribution of the binder on the fiber surface could be shown under the microscope. The resinized fibers were treated with the dye toluidine blue O to quench the autofluorescence of the wood fibers in order to show only the fluorescence of the UF resin in the presence of the dye. The results show that this method provides insight into the coverage of UF resin on wood fibers. However, the overall sample production time is long, additional dye needs to be added, and it is not suitable for rapid testing in production practice. Thumm et al. (2001) ground 1,4-bis[5-phenyl-2-oxazolyl]-benzene (POPOP) to a fine powder and mixed it into UF resin at a 5% load. After fracturing the panels by internal bonding tests, samples were taken from the exposed panel surfaces for inspection. The UF resin objects were made transparent by means of image processing software in order to view the underlying structure.

In contrast, hyperspectral techniques for the detection of UF resin content in fiberboard are relatively rare, but have relevant applications in other fields (Fujimoto et al. 2008, Kobori et al.

2013). Sun et al. (2003) investigated the curing process of glass-reinforced phenolic resin prepreg using NIR reflectance spectroscopy. A mathematical model between the NIR spectral parameters and the quality criteria (resin content and volatile content) of glass-reinforced phenolic resin prepreg was developed using principal component analysis (PCA), and the effect of analytical accuracy was investigated using principal component regression. The results showed that the correlation coefficient of the untreated spectral model for resin content was 0.9719 and 0.9675 after the first-order derivative treatment, thus verifying the feasibility of NIR analysis technique for testing the quality of composite prepreg.

Canaza-Cayo et al. (2013) used NIR reflectance spectroscopy (NIRS) in combination with multivariate analysis to assess the predicted textile quality attributes of alpaca fiber. Raw samples of fiber taken from male and female Huacaya alpacas of different ages and colours were scanned and their visible-near infrared (NIR; 400 to 2500 nm) reflectance spectra were collected and analysed. Patterns of spectral variation were explored by principal component analysis (PCA). Calibration models were built by modified partial least squares regression, testing different mathematical treatments of the spectra (derivative order, subtractive gaps, smoothed segments) and whether spectral correction algorithms (standard normal variables and dephasing) were applied. Thus confirming that NIRS can be used as an effective technique to select alpaca fiber based on some important textile quality characteristics.

CONCLUSIONS

The content of UF resin is an important process indicator in the production of fiberboard, which affects not only the mechanical properties of the fiberboard material, but also the adjustment of the hot pressing process parameters during the production of fiberboard. The precise control and quantitative detection of the urea-formaldehyde resin content in poplar fibers is a prerequisite for the qualified production of high-density ultra-thin fiberboard. This paper presents a new method for the rapid detection of UF resin content in poplar fibers based on near-infrared hyperspectral imaging, which is less costly than XPS detection, allows for rapid detection and is of great significance for the rapid feedback adjustment of gluing quantities in the industrial continuous production of fiberboard.

From the experimental data, it can be seen that the partial least squares regression (PLSR) model with MC, MSC, SNV and 1-Der pretreatments has different prediction performance, among which the full band SNV-PLSR model has the best performance with a correction coefficient of determination R^2c of 0.959, a prediction coefficient of determination R^2p of 0.937, a root mean square error of correction RMSEC of 0.805. 29 and 55 feature bands were extracted by SPA and CARS respectively, with the CARS model performing better with R^2c values of 0.941, R^2p values of 0.921, RMSEC values of 0.865 and RMSEP values of 1.305. This experimental study innovatively extends the method for the detection of UF resin content in poplar fibers, providing a theoretical reference and practical validation for the hyperspectral detection of UF resin content. The hyperspectral model can be further optimised for the rapid detection of urea-formaldehyde resin content in ultra-thin fiberboard production lines, thus providing data support for the subsequent adjustment of lay-up and hot pressing process parameters, which has important production implications.

ACKNOWLEDGMENTS

The study was funded by National Key R&D Program of the Ministry of Science and Technology of the People's Republic of China (2021YFD220060404) and Basic Scientific Research Funds of Central Universities (No.2572021BF03).

REFERENCES

1. Canaza-Cayo, A.W., Alomar, D., Quispe, E., 2013: Prediction of alpaca fibre quality by near-infrared reflectance spectroscopy. Animal, 7(7): 1219-1225.
2. Carvalho, Luisa M.H., Costa., Carlos A.V., 1998: Modeling and simulation of the hot-pressing process in the production of medium density fiberboard (MDF). Chemical Engineering Communications, 170(1):1-21.
3. Cleve, E., Bach, E., Schollmeyer E., 2000: Using chemometric methods and NIR spectrophotometry in the textile industry. Analytica Chimica Acta, 420:163-16.
4. Fujimoto, T., Kobori, H. and Tsuchikawa, S. 2012: Prediction of wood density independently of moisture conditions using near infrared spectroscopy. Journal of Near Infrared Spectroscopy, 20(3), 353–359.
5. Fujimoto, T., Kurata, Y., Matsumoto, K., Tsuchikawa, S. 2008: Application of near infrared spectroscopy for estimating wood mechanical properties of small clear and full length lumber specimens. Journal of Near Infrared Spectroscopy, 16(6), 529–537.
6. Fernandes, A., Lousada, J., Morais, J., Xavier, J., Pereira, J., Melo-Pinto, P., 2013: Measurement of intra-ring wood density by means of imaging VIS/NIR spectroscopy (hyperspectral imaging). Holzforschung, 67(1), 59-65.
7. Garcia, R.A., Cloutier, A., 2005: Characterization of heat and mass transfer in the mat during the hot pressing of MDF panels. Wood and Fiber Science, 37(1):23–41.
8. Hata, T., Kawai, S., Sasaki, H., 1989: Computer simulation of temperature behavior in particle mat during hot pressing and steam injection pressing. Wood Science and Technology, 23(4): 361–369.
9. Jakes, J.E., Frihart, C.R., Hunt, C.G., 2019: X-ray methods to observe and quantify adhesive penetration into wood. Journal of Materials Science, 54, 705–718.
10. Javed, M.A., Kekkonen, P.M., Ahola, S., Telkki, V.V., 2015: Magnetic resonance imaging study of water absorption in thermally modified pine wood. Holzforschung, 69(7), 899–907.
11. Jiang, B., Huang, Y.D., 2007: On-line monitoring of alkali-free cloth/phenolic resin prepreg by near-infrared spectroscopy. Journal of Reinforced Plastics and Composites, 26(16):1625-1636.
12. Kekkonen, P.M., Ylisassi, A., Telkki, V.V., 2014: Absorption of water in thermally modified pine wood as studied by nuclear magnetic resonance. Journal of Physical Chemistry C, 118(4), 2146–2153.
13. Kobori, H., Gorretta, N., Rabatel, G., Bellon-Maurel, V., Chaix, G., Roger, J.M., Tsuchika wa, S., 2013: Applicability of Vis-NIR hyperspectral imaging for monitoring wood moisture content (MC). Holzforschung, 67(3), 307–314.

14. Liu, D., Wang, L., Sun, D.W., Zeng, X.A., Qu, J.H ., Ma, J., 2014: Lychee variety discrimination by hyperspectral imaging coupled with multivariate classification. Food Analytical Methods, **7**: 1848–1857.
15. Liu, Z., Zhang, R., Zhang, G., Chen, K., 2016: Wavelength variable selection method in near infrared spectroscopy based on discrete firefly algorithm. Spectroscopy and Spectral Analysis, 36(12):3931–6.
16. Lorente, D., Aleixos, N., Gómez-Sanchis, J., Cubero, S., Blasco, J., 2013: Selection of optimal wavelength features for decay detection in citrus fruit using the ROC curve and neural networks. Food and Bioprocess Technology, 6:530–541.
17. Meng, F H., 2011: The optimization control study on parallel online mixing and supplying glue of MDF. Dissertation for the Degree of Master. Northeast Forestry University: 35-46.
18. Magwaza, L.S., Opara, U.L., Nieuwoudt, H, Cronje, P.J.R., Saeys, W., Nicolaï, B., 2012: NIR spectroscopy applications for internal and external quality analysis of citrus fruit – a review. Food and Bioprocess Technology, 5(2):425–444.
19. Ma, T., Inagaki, T., Tsuchikawa S., 2018: Non-destructive evaluation of wood stiffness and fiber coarseness, derived from SilviScan data, via near infrared hyperspectral imaging. Journal of Near Infrared Spectroscopy, 26(6):398-405.
20. Ncube E., 2012: Predicting thickness swelling of hot-pressed wood strands. Bioresources, 7(2):5-8.
21. Özparpucu, M., Windeisen-Holzhauser, E., Wegener, G., 2022: A new analytical approach to investigate the influence of wood extracts on the curing properties of phenol-resorcinol–formaldehyde (PRF) adhesives. Wood Science and Technology, 56, 349–365.
22. Reis, C.A., Cisneros, A.B., da Silva, E.L., de Muñiz, G.I.B., Morrone, S.R., Nisgoski., S., 2019: NIR spectroscopy and wood anatomy to distinguish Prosopis alba wood and charcoal from natural and planted forest. International Wood Products Journal, 10(4):168–177.
23. Rofii, M.N., Yamamotoo, N., Ueda, S., 2014: The temperature behaviour inside the mat of wood-based panel during hot pressing under various manufacturing conditions. Journal of Wood Science, 60(6):414-420.
24. Shao, Y.Y., Wang, Y.X., Xuan, G.T., Gao, Z.M., Liu, Y., Han, X., Gao, Ch., 2019: Rapid detection of soluble solids content in strawberry coated with chitosan based on hyperspectral imaging. Transactions of the Chinese Society of Agricultural Engineering, 35(18):245-254.
25. Stefansson, P., Thiis, T., Gobakken, L.R., Ingunn, B., 2021: Hyperspectral NIR time series imaging used as a new method for estimating the moisture content dynamics of thermally modified Scots pine. Wood Material Science & Engineering, 16 (1):49.
26. Sun, Y. F., Huang, Y.D., Wang, Ch., 2003: Application of PCA for quantitativing the resin and volatile content of glass-fiber reinforced phinolic resin prepreg by near infrared spectroscopy. Journal of Aeronautical Materials, 23(1): 52-56.
27. Tang, Q.H., Zou, M., XU, Sh.D., Zhu, Y.B., Zhang, L., Guo, W.J., Chang, L., 2022: Effect of lsocyanate resin content on properties of high-density fiberboards. Chinese Journal of Wood Science and Technology, 36(03):40-45.

28. Thoemen, H., Humprey, P.E., 2003: Modeling the continuous pressing process for wood-based composites. Wood and Fiber Science. 35(3): 456–468.
29. Thoemen, H., Haselein, C.R., Humprey, P.E., 2006: Modeling the physical processes relevant during hot pressing of wood-based composites. Part II. Rheology. European Journal of Wood and Wood Products. 64(2):125-133.
30. Tsuchikawa, S., Kobori, H., 2015: A review of recent application of near infrared spectroscopy to wood science and technology. Journal of Wood Science, 61, 213–220.
31. Thumm, A., McDonald, A.G., Donaldson, L.A., 2001: Visualisation of UF resin in MDF by cathodoluminescent/scanning electron microscopy. European Journal of Wood and Wood Products, 59:215–216.
32. Xing, C., Riedl, B., Cloutier, A., 2004: Measurement of urea-formaldehyde resin distribution as a function of MDF fiber size by laser scanning microscopy. Wood Science and Technology, 37(6):495–507.
33. Xing C., Riedl B., Cloutier A., Shaler S.M., 2005: Characterization of UF resin penetration into MDF fibers. Wood Science and Technology, 39(5):374–384.
34. Zhu, Q., Huang, M., Zhao, X., Wang, S.H., 2013: Wavelength selection of hyperspectral scattering image using new semi-supervised affinity propagation for prediction of firmness and soluble solid content in apples. Food Analytical Methods, 6:334–342.
35. Zhang, L., Zou, M., Tang, Q.H., Guo, W.J., 2023: Effects of hot-pressing time and temperature on properties of phenolic resin ultra-thin high density fiberboards. Chinese Journal of Wood Science and Technology, 37(01):68-73.
36. Zou, M., Guo, W.J., Tang, Q.H., 2020: Effect of density and resin content on bending strength and water resistance of high-density fiberboard. Chinese Journal of Wood Science and Technology, 34(06):11-14+19.

CHUNMEI YANG[1], ZANBIN ZHU[1,2]*, TONGBIN LIU[1], BO XUE[1]*,
WEN QU[1]*, TINGTING WANG[1]
[1]NORTHEAST FORESTRY UNIVERSITY
COLLEGE OF MECHANICAL AND ELECTRICAL ENGINEERING
HARBIN 150040
CHINA
[2]XINYANG AGRICULTURE AND FORESTRY UNIVERSITY
XINYANG 464000
CHINA
*Corresponding authors: zlx20063500@126.com, xuebo@nefu.edu.cn and qwnefu@126.com